Black Sea Journal of Engineering and Science
doi: 10.34248/bsengineering.1592949

Open Access Journal
e-ISSN: 2619 – 8991

Araştırma Makalesi (Research Article)
Cilt 8 - Sayı 2: XX-XX / Ay Yıl
(Volume 8 - Issue 2: XX-XX / Month Year)

UTILIZATION OF WASTE HEAT IN CLOSED BRAYTON CYCLE: A THERMODYNAMIC ANALYSIS WITH VARIOUS WORKING FLUIDS

Gamze SOYTÜRK[1]*

[1]*Isparta University of Applied Sciences, Faculty of Technology, Department of Mechanical Engineering, 32200, Isparta, Turkey*

Abstract: This research investigates the thermodynamic performance of a power generation system employing five working fluids: helium, carbondioxide, nitrogen, argon, and neon. Key parameters like net power generation, exergy destruction, energy and exergy efficiencies, and mass flow rates were evaluated under varying operational conditions. The analysis revealed that carbondioxide consistently outperformed other fluids, achieving the highest net power generation of 450 kW at lower compressor inlet temperatures, and maintaining the lowest exergy destruction of approximately 500 kW. Additionally, carbondioxide exhibited superior energy and exergy efficiencies, with values reaching 31% and 45%, respectively. Nitrogen and argon demonstrated moderate performance, with nitrogen achieving a stable net power generation of around 250 kW and an exergy destruction of approximately 700 kW. Both fluids-maintained energy efficiencies near 17% and exergy efficiencies of approximately 25%, making them suitable for balanced thermodynamic systems. In contrast, neon and helium showed limited performance, with neon recording the lowest net power generation of 170 kW and a relatively high exergy destruction of 770 kW. Helium similarly exhibited reduced efficiencies, with energy efficiency dropping to 13% and exergy efficiency to 19% under varying conditions. Mass flow rate analysis indicated argon required the highest flow, at approximately 9.5 kg/s, while helium maintained the lowest at 1 kg/s, reflecting their respective densities and energy transport capacities. These findings underline the critical role of working fluid selection, with carbondioxide emerging as the optimal choice for systems prioritizing high efficiency and minimal energy losses. The study provides a comprehensive framework for enhancing thermodynamic performance in power generation applications.

Keywords: Waste heat recovery, Power generation systems, Working fluids, Thermodynamic analysis

***Corresponding author:** Isparta University of Applied Sciences, Faculty of Technology, Department of Mechanical Engineering, 32200, Isparta, Turkey
E mail: gamzeyildirim@isparta.edu.tr (G. SOYTÜRK)
Gamze SOYTÜRK https://orcid.org/ 0000-0001-7191-8765

Received: November 29, 2024
Accepted: January 7, 2025
Published: March 15, 2025

Cite as: Soytürk G. 2025. Utilization of waste heat in closed Brayton cycle: A thermodynamic analysis with various working fluids. BSJ Eng Sci, 8(2): xx-xx.

1. Introduction

The need to reduce environmental effects and the growing demand for energy worldwide have made improving power generation systems' efficiency even more important. A critical aspect of this enhancement lies in the selection of appropriate working fluids, which significantly influence the thermodynamic performance of these systems. Closed-cycle gas turbines and Organic Rankine Cycles (ORCs) have emerged as viable technologies for harnessing energy from diverse sources, including waste heat, liquefied natural gas (LNG), and industrial processes. In addition to increasing energy efficiency, these technologies are essential for lowering greenhouse gas emissions and halting climate change.

In addition to being a crucial strategy for advancing the shift to a low-carbon economy and meeting climate targets, industrial waste heat recovery, or WHR, is also a vital step in fostering sustainable growth and protecting the environment. In energy-intensive industries such as iron and steel production, waste heat represents a substantial untapped energy resource. Research has shown that waste heat recovery systems integrated with ORCs can transform low, medium, and high-temperature heat sources into electricity, significantly enhancing energy efficiency and reducing carbon emissions. For instance, the iron and steel industry alone accounts for nearly 5% of global energy consumption, making it a prime candidate for waste heat recovery solutions. Studies have demonstrated that ORCs can efficiently utilize heat sources below 400°C, converting waste energy into usable electricity, thereby reducing reliance on external power grids. A research by Campana et al. (2013) assessed the potential for energy savings and the reduction of CO_2 emissions using ORC systems in conjunction with industrial waste heat recovery. In the most promising industrial sectors of the 27 EU member states, they reported that ORC technology might save 20.000 GWh of energy annually and reduce CO_2 emissions by 7.6 Mt. Chen et al. (2016) investigated the potential of ORCs to generate energy from the surplus heat present at UK industrial sites that participate in the EU ETS. The findings demonstrated that raising the temperature of the available heat source boosts the Carnot efficiency. According to Petr and Raabe (2015), R1234ze(Z) has

favourable thermophysical characteristics and may be a viable substitute for R245fa in an ORC system in conjunction with an industrial waste heat recovery system, where the heat source temperature ranges from 183℃ to 224℃ The parametric evaluation of the ORC was carried out by D.K. Kim et al. (2017) utilizing R245fa as the working fluid and a low-grade waste heat below 80 °C. He discovered that at a heat source temperature of 80 °C, the system can produce 411.3W with an efficiency of 3.6%.

Recent advancements in thermodynamic cycle design, such as the incorporation of real gas Brayton cycles, have further expanded the potential for waste heat recovery (Farrukh et al., 2023). By selecting working fluids like nitrogen and carbondioxide, which exhibit favourable critical properties, these systems can maximize energy recovery while minimizing exergy destruction. These innovations are particularly relevant for applications involving cryogenic energy utilization and high-efficiency waste heat recovery (Jafari et al., 2023). In order to attain greater thermal efficiency, Xu and Yu (2014) suggested R245fa and R141b as the ideal working fluids, highlighting the importance of the critical temperature as a determining factor in fluid selection. According to their recommendations, the crucial temperature should be between 30 and 100 K below the waste gas inlet 5 temperature, respectively. Using low-grade waste heat at 85 °C, Zhao et al. (2012) examined the system parameters with various working fluids and concluded that R123 was an efficient working fluid in terms of high thermal efficiency and turbine power production. A new kind of cogeneration system for collecting gas turbine waste heat was proposed by Li et al. (2020). The results demonstrated that the energy efficiency improved by 4.62% to a maximum of 52.53% when the turbine input temperature was 375.4°C. The effects of system parameters (heat storage temperature, temperature difference, and component efficacy) and heat source conditions (flow rate and temperature) were assessed by In their thermodynamic model of a system, Hu et al. (2021) used solar energy, waste heat, and a district heating network. Andreasen et al. (2014) published an approach for selecting the working fluid for an ORC unit that employs low-temperature heat. After the ORC unit was optimized, thirty pure and mixed working fluids were chosen. To recover low-grade waste heat, Yang et al. (2019) suggested a system that combines the absorption refrigeration cycle (ARC) waste heat recovery system with a transcritical CO_2 cycle. According to the findings, the suggested solution performed better at lower ARC refrigeration temperatures. The effectiveness of an ARC system powered by ship waste heat for refrigeration was examined by Salmi et al. (2017). The LiBr-water working pair was more effective than the others, according to the results. Additionally, recovering the waste heat for cooling resulted in a 70% reduction in compressor power consumption. Hajabdollahi et al. (2013) conducted a thermo-economic optimization study that focused on the overall cost and thermal efficiency for diesel waste heat. Their findings indicated that R123 was the best working fluid; R245fa showed comparable results. Mocanu et al. (2024) investigated the reduction of waste heat from the exhaust gas of the internal combustion engine in a series of diesel-electric hybrids buses. They compared the performance of the split-flow supercritical CO_2 recompressions Brayton cycle with the steam Rankine and Organic Rankine cycles by examining the heat recovery and conversion into useful power of the Brayton cycle. Alzuwayer et al. (2024) introduced a cascade system that uses exhaust gases from a marine gas turbine propulsion system as a heat source for the bottom supercritical CO_2 Brayton cycle. The study focused on recompression cycle schemes by analyzing parameters such as CO_2 mass flow rate and the efficiency of low-temperature and high-temperature recuperators to improve the overall system efficiency. Rad et al. (2024) studied the feasibility of utilizing waste heat from refinery exhaust flares by interesting a closed Brayton cycle with an ORC and an absorption cooler. In this research, they analyzed various working fluids including air, helium, oxygen, carbon dioxide, xenon, and nitrogen to improve the system performance through parametric studied and optimization.

Despite these advancements, there remains a critical need for a more comprehensive and systematic comparison of fluids across a broader range of operational conditions to better understand their behaviour and performance. Key factors, such as PR (PR), turbine inlet temperature, and compressor inlet temperature, play pivotal roles in determining the overall efficiency, power output, and thermodynamic effectiveness of power generation systems. Variations in these parameters can significantly influence fluid properties, such as specific heat capacity and thermal conductivity, thereby impacting energy conversion efficiency and exergy destruction. A deeper analysis of how each working fluid responds to these changes is essential for optimizing system design, ensuring robust performance, and tailoring solutions to meet the demands of specific industrial applications and waste heat recovery scenarios. This approach can help bridge existing knowledge gaps and provide a foundation for improving the energy efficiency and sustainability of advanced power generation cycles.

The purpose of this paper is to evaluate and compare the thermodynamic performance of a power generation system utilizing five different working fluids—helium, carbondioxide, nitrogen, argon, and neon—under various operating conditions. By analysing key metrics such as net power generation, exergy destruction, energy and exergy efficiencies, and mass flow rates, the study aims to identify the optimal working fluid for maximizing system efficiency and minimizing energy losses. The originality of this research lies in its comprehensive examination of multiple thermodynamic parameters across a wide range of conditions, offering detailed insights into the performance trade-offs associated with each fluid. Unlike previous studies, this work integrates the effects of

turbine inlet temperature, compressor inlet temperature, and PR into a unified framework, providing a robust comparison of fluid suitability for advanced power generation systems. This approach not only highlights the critical role of fluid selection in improving system efficiency but also contributes valuable data for optimizing the design and operation of thermodynamic cycles.

2. Materials and Methods

2.1. System Description

Figure 1 illustrates a complex thermodynamic cycle, likely representing a combined Brayton and Rankine cycle, which is optimized for efficient energy generation. The system integrates multiple compression and expansion stages, heat exchangers, and a recuperator to enhance thermal efficiency. Starting from the left, ambient air enters the first compressor (C1) and undergoes sequential compression through compressors (C2 and C3), with intercoolers (IC1 and IC2) placed between the stages to reduce the work of compression. After compression, the air flows through a gas cooler (GC) and a recuperator (REC), where waste heat from the cycle is recovered to preheat the working fluid. This preheated air is directed to the combustion chamber, where it mixes with fuel, and the high-temperature flue gases expand through the turbines (T1 and T2), generating mechanical power, which is converted into electricity via a generator. The waste heat from the flue gases is captured in a heat recovery steam generator section, shown as a flue gas heat exchanger, further improving system efficiency by transferring residual heat to other cycle components or processes. The integration of heat exchangers, intercoolers, and the recuperator emphasizes the system's focus on energy recovery and minimization of losses. The flue gases are eventually released after maximizing heat extraction, contributing to overall cycle efficiency. This system demonstrates an advanced thermodynamic design that balances power generation, waste heat recovery, and operational sustainability.

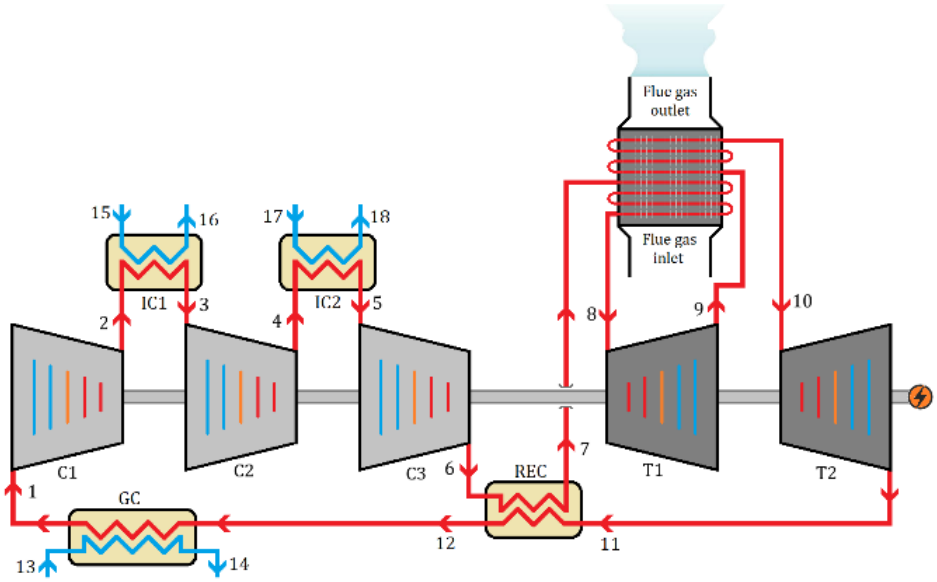

Figure 1. Schematic of a thermodynamic cycle with multi-stage compression, intercooling, recuperation, and dual-stage expansion.

2.2. Working Fluid Selection

The thermodynamic properties of the fluids considered in this research are summarized in the table 1, showcasing key parameters such as molecular mass, critical temperature, and critical pressure. These fluids include nitrogen, air, argon, oxygen, and methane, which are commonly used in various energy and cryogenic systems due to their unique physical characteristics. Nitrogen and air, with relatively low critical temperatures and pressures, are ideal for applications involving low-temperature processes. Argon and oxygen, with higher critical temperatures and pressures, are suitable for systems requiring efficient heat transfer and stable thermodynamic behavior under high-pressure conditions. Methane, characterized by its low molecular mass and moderately high critical temperature, is widely used in energy applications, particularly in power generation and refrigeration cycles. The diverse properties of these fluids allow for their application in a range of thermodynamic cycles, enabling optimized performance for specific operational requirements.

Table 1. Thermodynamic properties of selected working fluids (Angelino and Invernizzi, 2011)

Fluid	Molecular mass (g/mol)	Critical temperature (K)	Critical pressure (bar)
Nitrogen	28.014	126.2	33.98
Air	28.96	132.52	37.66
Argon	39.948	150.86	48.98
Oxygen	31.999	154.58	50.43
Methane	16.043	190.56	45.99

2.3. Thermodynamic Analysis

Establishing the equalities for mass, energy, entropy, and exergy balances is the first stage in thermodynamic evaluation (Arslan and Yılmaz, 2022). Determining characteristics such as the inlet and output power and heat rates, the entropy creation and destruction rates, and providing a summary of the energetic performance of the studied thermodynamic process all require it. This study will explore various modeling methodologies, beginning with the general balance equations of mass and energy and moving on to exergy analysis (Yılmaz et al., 2019). The following primary presumptions form the basis of this study's thermodynamic analysis:

•All system components are chosen to function in both steady-state and steady-flow scenarios; the reference state is taken to be 25°C and 101.325 kPa of pressure.

•Pump and turbine heat losses are not considered.

•When thinking about energy changes, the changes in potential and kinetic energies are neglected.

For a steady-state control volume, the general balance equation of mass is (Cengel and Boles, 2015):

$$\sum \dot{m}_{in} = \sum \dot{m}_{out} \quad (1)$$

The energy balance equation is as follows:

$$\sum \dot{E}_{in} = \sum \dot{E}_{out} \quad (2)$$

The subscripts "*in*" and ""*out*" in equations 1 and 2 indicate the inlet and exit points of the control volume, whereas $\dot{m}$ stands for the mass flow rate and $\dot{E}$ for the energy rate. According to Cengel and Boles, (2015) the energy balance equation is changed by adding heat and work factors to these equations:

$$\dot{Q} + \sum \dot{m}_{in} h_{in} = \dot{W} + \sum \dot{m}_{out} h_{out} \quad (3)$$

$\dot{Q}$ is the heat in the equation above, and $\dot{W}$ is the work.

The exergy balance is calculated as follows to perform a second law analysis of the plant (Dincer and Rosen, 2013):

$$\sum \dot{E}x_{in} = \sum \dot{E}x_{out} + \sum \dot{E}x_{dest} \quad (4)$$

In this case, $\dot{E}x$ denotes the rate of exergy and $\dot{E}x_{dest}$ denotes the rate of exergy destruction. Equation (5) can be written as follows by adding more exergy terms:

$$\dot{E}x_Q - \dot{E}x_W = \sum \dot{m}_{out} e_{out} - \sum \dot{m}_{in} e_{in} + T_0 \dot{S}_{gen} \quad (5)$$

The exergy associated with heat is represented by $\dot{E}x_Q$ in the above equation, the exergy associated with work by $\dot{E}x_W$, and the thermo-physical flow exergy by e. Entropy generation is shown by the equation's last term, $\dot{S}_{gen}$, which has the following definition (Bejan et al., 1996):

$$\dot{E}x_{dest} = T_0 \dot{S}_{gen} \quad (6)$$

The following formulas could be used to calculate the thermo-physical flow exergy and the exergy associated with heat and work (Dincer and Rosen, 2013):

$$\dot{E}x_Q = \dot{Q}\left(\frac{T - T_0}{T}\right) \quad (7)$$

$$\dot{E}x_W = \dot{W} \quad (8)$$

$$e = (h - h_0) - T_0(s - s_0) \quad (9)$$

where *h* stands for the specific enthalpy, *s* for the specific entropy, and the subscript *0* for reference circumstances.

Exergy efficiency is expressed as follows:

$$\eta_{ex} = \frac{\dot{W}_{net}}{\dot{E}x_{\dot{Q},in}} \quad (10)$$

Here $\dot{W}_{net}$ shows for the net power, $\dot{E}x_{\dot{Q},in}$ for exergy of net heat rate.

3. Results

This section presents the findings of a comprehensive thermodynamic analysis performed on a power generation system using five different working fluids: helium, carbondioxide, nitrogen, argon, and neon. The results are analyzed across varying operational conditions, including PR, turbine inlet temperature, and compressor inlet temperature, to evaluate their impact on key performance metrics. These metrics include net power generation, energy and exergy efficiencies, exergy destruction, and mass flow rates. The findings provide valuable insights into the comparative performance of the working fluids, highlighting their suitability for optimizing power generation systems and waste heat recovery processes. Table 2 provides key operational parameters and reference values used in the thermodynamic analysis of the power generation system. These parameters serve as the baseline for evaluating system performance and comparing the working fluids.

Table 2. Operational parameters and reference values for the thermodynamic analysis of the power generation system (Farrukh et al., 2023)

Parameters	Value
Reference temperature	25℃
Reference pressure	101.3 kPa
Total waste heat	1500 kW
Source temperature	650 ℃
Turbine inlet temperature	350 ℃
Compressor inlet temperature	35 ℃
Pressure ratio	3.5
Effectiveness recuperator	0.65
Compressor isentropic efficiency	0.85
Compressor isentropic efficiency	0.88

Figure 2 presents the comparison of net power generation (blue bars) and exergy destruction (orange bars) for various working fluids: helium, carbondioxide, nitrogen, argon, and neon. The results provide insight into the performance and efficiency of these fluids in the described thermodynamic system. Helium and neon exhibit the lowest levels of net power generation (helium 191.2 kW, neon 185.6 kW), with neon producing even less power than helium. This indicates that neon is less effective as a working fluid in this system configuration. However, both fluids also demonstrate relatively high levels of exergy destruction (helium 751.7 kW, neon 712.8 kW), suggesting

significant thermodynamic inefficiencies. Carbondioxide, on the other hand, shows the highest net power generation (437.1 kW) among the fluids, albeit with substantial exergy destruction. This highlights its strong potential for power generation but also points to room for improvement in reducing energy losses. Nitrogen and argon show moderate levels of net power generation compared to carbondioxide, with nitrogen slightly outperforming argon (nitrogen 247.3 kW, argon 231.1 kW). However, both fluids have lower exergy destruction compared to neon and helium, indicating a better balance between power generation and efficiency. Overall, the chart demonstrates the importance of selecting the appropriate working fluid based on system objectives. While carbondioxide excels in power generation, reducing its exergy destruction could further enhance its efficiency. Argon and nitrogen appear to provide a more balanced performance, whereas helium and neon are less suitable for achieving high net power output in this system.

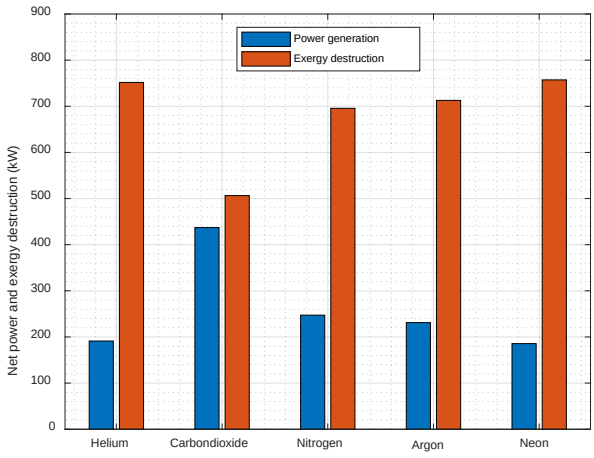

Figure 2. Comparison of net power generation and exergy destruction for different working fluids in the thermodynamic cycle.

Figure 3 displays the energy and exergy efficiencies for helium, carbondioxide, nitrogen, argon, and neon, providing a clear comparison of their performance in the thermodynamic system. The numerical values of these efficiencies, as derived from the chart, offer additional clarity. Carbondioxide stands out with the highest efficiency values, achieving an energy efficiency of 31.22% and an exergy efficiency of 45.75%. This demonstrates its strong potential to effectively convert energy while minimizing irreversibilities in the process. Nitrogen and argon follow with moderate performance, where nitrogen has an energetic efficiency of 17.66% and an exergetic efficiency of 25.88%, and argon shows similar values with an energy efficiency of 16.5% and an exergy efficiency of 24.18%. These results highlight the balanced performance of nitrogen and argon, where a significant portion of energy is effectively utilized at higher thermodynamic quality levels. Helium and neon show considerably lower efficiencies. Helium achieves an energetic efficiency of only 13.66% and an exergetic efficiency of 20%, making it the least efficient working fluid in this system. Neon performs slightly better, with an energy efficiency of 13.26% and an exergy efficiency of 19.43%, but it still falls short compared to carbondioxide, nitrogen, and argon. In summary, carbondioxide clearly emerges as the most efficient fluid in terms of energy and exergy utilization. Nitrogen and argon provide moderate efficiency and could serve as alternatives for systems requiring balanced performance. Helium and neon, however, exhibit poor efficiencies, indicating their limited suitability for high-performance thermodynamic systems. These quantitative findings underline the critical role of fluid selection in achieving optimal system performance.

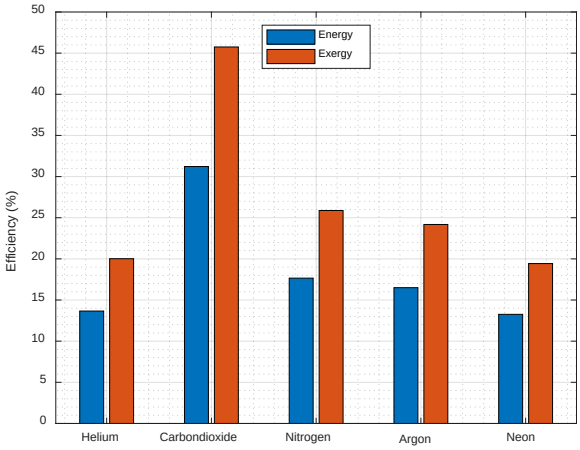

Figure 3. Energy and exergy efficiencies of different working fluids in the thermodynamic system.

Figure 4 illustrates the exergy destruction within various system components for five working fluids: helium, carbondioxide, nitrogen, argon, and neon. Each bar represents the contribution of a specific component—compressors, intercoolers, heat exchangers, gas cooler, recuperator, and turbines—to the general exergy destruction of the plant. Among all working fluids, the heat exchanger labelled HE1 contributes the highest exergy destruction, around 250 kW per fluid. This suggests that HE1 is the primary source of irreversibilities within the system and a critical target for efficiency improvement. Similarly, the gas cooler (GC) and HE2 also show significant exergy destruction, particularly for helium, nitrogen, and neon, emphasizing their substantial impact on system losses. The compressors (C1, C2, C3) and intercoolers (IC1, IC2) exhibit comparatively lower exergy destruction. Among these, C3 shows a slightly higher exergy destruction for most fluids, especially for carbondioxide and neon, while the other compressors and intercoolers contribute minimally. The turbines (T1, T2) show relatively low levels of exergy destruction across all fluids, highlighting their efficient performance compared to the other components. The recuperator (REC) displays moderate exergy destruction, with its contribution being slightly higher for carbondioxide and nitrogen.

Overall, the chart demonstrates that heat exchangers, particularly HE1, are the dominant contributors to exergy

destruction in the plant, followed by GC and HE2. Compressors, intercoolers, turbines, and the recuperator contribute significantly less, making them less critical for optimization efforts. This analysis highlights the importance of targeting heat exchanger performance improvements to reduce overall system losses and enhance efficiency.

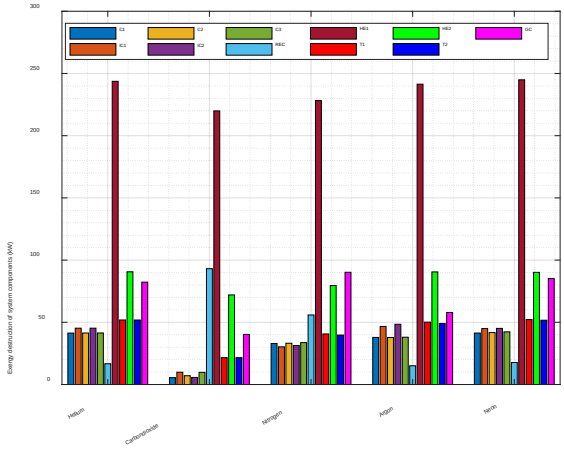

Figure 4. Exergy destruction distribution among system components for various working fluids.

Figure 5 represents the mass flow rates of various working fluids—helium, carbondioxide, nitrogen, argon, and neon—used in the thermodynamic system. Each fluid exhibits a distinct flow rate, reflecting differences in their thermodynamic and physical properties. Argon has the highest mass flow rate, reaching approximately 9 kg/s, which indicates its significant role in maintaining the system's energy transfer requirements. This is likely due to its higher density and favorable thermophysical characteristics. Nitrogen and carbondioxide follow with moderate mass flow rates, around 5.5 kg/s and 5 kg/s, respectively. These values suggest their balanced performance in terms of mass requirements to achieve desired thermodynamic outputs.

Neon, with a flow rate close to 5 kg/s, performs slightly below nitrogen. Helium exhibits the lowest mass flow rate, slightly above 1 kg/s, indicating its lower density and specific energy transfer capacity compared to the other fluids. This variation in mass flow rates highlights the dependency of system design on the chosen working fluid. Higher mass flow rates, as seen in argon, may require larger component dimensions and higher pumping power, whereas lower flow rates, like helium, could result in reduced equipment size but potentially lower system efficiency.

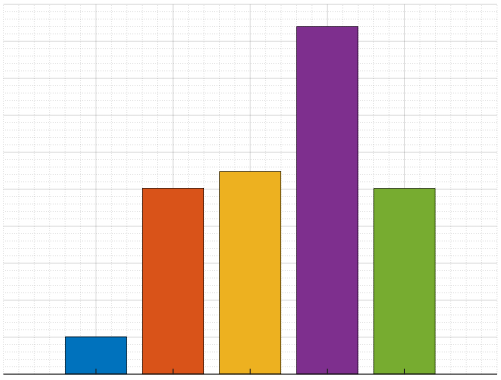

Figure 5. Mass flow rates of working fluids in the thermodynamic system.

Figure 6 illustrates the effect of turbine inlet temperature on the net power production for selected fluids. As seen in the figure, carbondioxide consistently achieves the highest net power generation, starting at approximately 420 kW at 300°C and increasing to nearly 450 kW at 400°C. This demonstrates its excellent thermal performance and suitability for high-temperature applications. Nitrogen and argon show similar trends, with nitrogen slightly outperforming argon. At 300°C, nitrogen generates approximately 190 kW, rising to around 300 kW at 400°C. Argon starts at approximately 150 kW at 300°C and increases to around 300 kW at 400°C. These results suggest their moderate performance, suitable for applications where a balance of efficiency and output is required. Neon exhibits lower power generation compared to nitrogen and argon, starting at about 100 kW at 300°C and increasing to roughly 250 kW at 400°C. This indicates its limited capability for high-efficiency energy conversion under these conditions. Helium consistently shows the lowest net power generation, beginning at 100 kW at 300°C and increasing to approximately 260 kW at 400°C. Its low density and specific energy transfer capacity limit its performance in this system. Overall, the chart emphasizes that higher turbine inlet temperatures significantly improve net power generation for all fluids. Carbondioxide clearly outperforms the others, making it the most effective working fluid, while helium and neon display the lowest performance. This analysis underscores the importance of fluid selection and operating conditions in optimizing system performance.

Figure 7 demonstrates the variation of exergy destruction with turbine inlet temperature for five working fluids. The results demonstrate that exergy destruction decreases with increasing turbine inlet temperature for all fluids, indicating improved thermodynamic efficiency at higher temperatures. Neon and Helium exhibit the highest exergy destruction across the temperature range, starting at approximately 850 kW and 840 kW at 300°C, respectively, and decreasing to around 680 kW and 670 kW at 400°C. These results reflect significant thermodynamic irreversibilities for these fluids in the system. Argon and

nitrogen show intermediate levels of exergy destruction. Argon starts at about 800 kW at 300°C and decreases to 650 kW at 400°C. Similarly, nitrogen begins at 760 kW and reduces to approximately 650 kW over the same temperature range. These fluids demonstrate a better balance between energy transfer and irreversibilities compared to helium and neon. Carbondioxide achieves the lowest exergy destruction, starting at around 520 kW at 300°C and slightly decreasing to about 490 kW at 400°C. This highlights carbondioxide's efficiency and its ability to minimize energy losses in the system.

Figure 8 depicts how energy efficiency changes with turbine inlet temperature for working fluids. A clear upward trend is observed for all fluids, indicating improved energy efficiency as the turbine inlet temperature increases. Carbondioxide consistently shows the highest energy efficiency, starting at around 30% at 300°C and increasing slightly to 32% at 400°C. This stable performance highlights its strong thermodynamic properties and suitability for efficient energy conversion. Nitrogen and argon display similar efficiency trends, with nitrogen slightly outperforming argon. Nitrogen's energy efficiency ranges from about 13% at 300°C to nearly 21% at 400°C, while argon's efficiency increases from 11% to approximately 21% over the same temperature range. These fluids provide balanced performance, suitable for moderate efficiency requirements. Neon shows lower energy efficiency compared to nitrogen and argon, starting at approximately 7% at 300°C and rising to 18% at 400°C. This demonstrates its limited potential for high-efficiency energy systems under these conditions. Helium has the lowest energy efficiency, beginning at 8% at 300°C and reaching about 19% at 400°C. Its performance is constrained by its low density and limited thermodynamic efficiency in this configuration.

The exergy efficiency variations of working fluids across a turbine inlet temperature range of 300°C to 400°C are shown in the figure 9. A general trend of increasing exergy efficiency with higher turbine inlet temperatures is observed for all fluids. Carbondioxide outperforms the other fluids by maintaining the highest exergy efficiency throughout the temperature range. Starting at approximately 44% at 300°C, its efficiency slightly increases to 47% at 400°C. This highlights its superior thermodynamic properties and minimal energy losses. Nitrogen and argon achieve intermediate efficiencies, with nitrogen slightly leading. Nitrogen's exergy efficiency rises from around 19% at 300°C to 31% at 400°C. Similarly, argon shows an improvement from 15% to approximately 31%. These results suggest both fluids provide a balanced level of performance suitable for moderate efficiency systems. Among the fluids, neon exhibits the lowest exergy efficiency, starting at approximately 10% at 300°C and rising to about 26% at 400°C, slightly lower than helium, which starts at 11% and reaches around 27%. This highlights neon's higher irreversibility compared to helium and the other fluids.

Figure 10 illustrates the mass flow rate trends for fluids as a function of turbine inlet temperature, ranging from 300°C to 400°C. It is evident that the mass flow rate decreases slightly with increasing temperature for all fluids. Argon consistently shows the highest mass flow rate, starting at approximately 10.4 kg/s at 300°C and decreasing to around 8.2 kg/s at 400°C. This indicates its significant density and energy transport capacity in the system. In the figure, nitrogen exhibits a moderate mass flow rate compared to the other working fluids. At a turbine inlet temperature of 300°C, nitrogen's mass flow rate starts at approximately 6.4 kg/s. As the temperature increases to 400°C, its flow rate decreases slightly, settling at around 5 kg/s. Carbondioxide and neon exhibit quite similar mass flow rates, starting at around 6 kg/s at 300°C and decreasing slightly to approximately 4.5 kg/s at 400°C. These fluids demonstrate moderate performance in terms of flow requirements. Helium shows the lowest mass flow rate, remaining nearly constant at around 1.2 kg/s throughout the temperature range. This reflects its low density and relatively low energy transfer capacity.

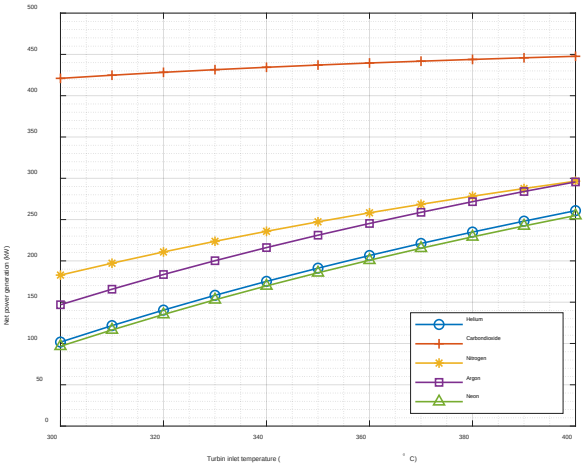

Figure 6. Effect of turbine inlet temperature on net power generation.

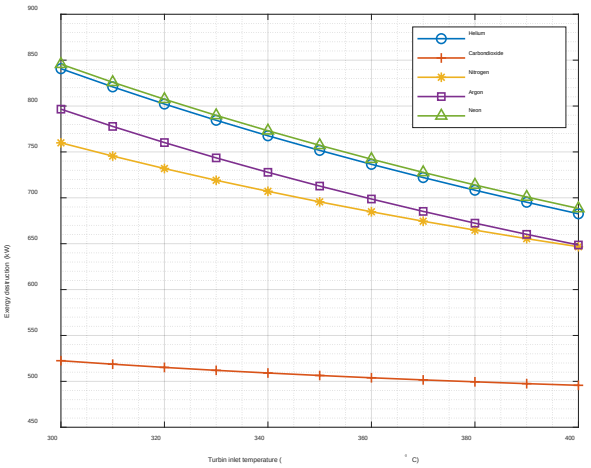

Figure 7. Effect of turbine inlet temperature on exergy destruction.

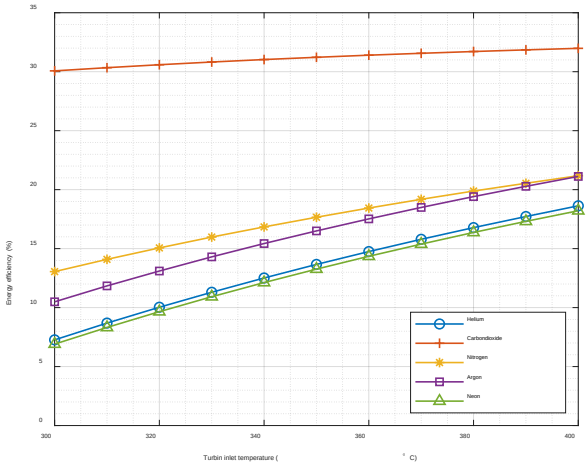

Figure 8. Effect of turbine inlet temperature on energy efficiency.

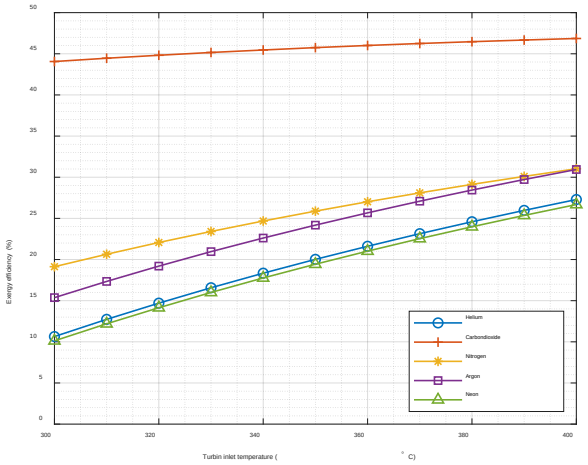

Figure 9. Effect of turbine inlet temperature on exergy efficiency.

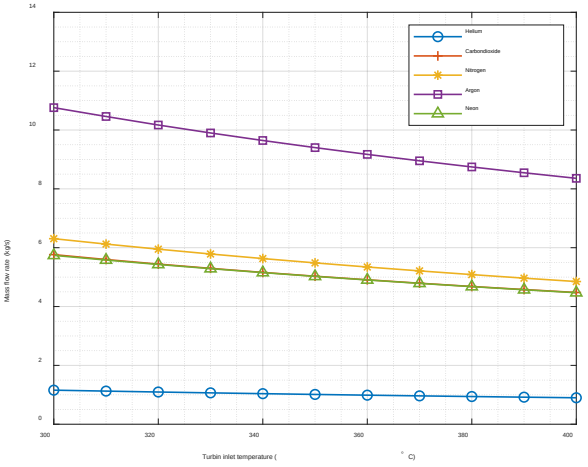

Figure 10. Effect of turbine inlet temperature on mass flow rate.

Figure 11 demonstrates the relationship between PR and net power generation for five working fluids: helium, carbondioxide, nitrogen, argon, and neon. The data demonstrates how net power output changes as the system's PR increases from 3 to 4. Carbondioxide consistently achieves the highest net power generation, starting at approximately 410 kW at a PR of 3 and increasing slightly to around 450 kW at a PR of 4. This highlights its superior thermodynamic performance and ability to effectively utilize higher PRs for power generation. Nitrogen maintains a nearly constant net power generation of around 250 kW across the entire PR range. Argon shows a slight decline in net power generation, starting at about 250 kW at a PR of 3 and decreasing to around 210 kW at a PR of 4. Neon and helium show lower power generation levels compared to the other fluids. Neon starts at approximately 210 kW at a PR of 3 and decreases to about 160 kW at a PR of 4. Similarly, helium exhibits a slight decline, beginning at around 210 kW and dropping to approximately 170 kW.

Figure 12 presents the exergy destruction trends for five working fluids over a range of PRs from 3 to 4. The results show varying behaviors, with carbondioxide exhibiting a decreasing trend, while the other fluids show either slight increases or consistent values. Carbondioxide demonstrates the lowest exergy destruction among all fluids, starting at approximately 540 kW at a PR of 3 and decreasing to about 490 kW at a PR of 4. This trend highlights its efficiency in minimizing energy losses as the PR increases, making it the most thermodynamically favorable working fluid in this analysis. Nitrogen and argon exhibit intermediate exergy destruction values, with nitrogen remaining nearly constant at approximately 700 kW throughout the PR range. Argon shows a slight increase from 700 kW at a PR of 3 to around 730 kW at 4. These fluids indicate moderate performance with stable irreversibilities. Helium and neon have the highest exergy destruction levels, starting at approximately 735 kW for helium and 740 kW for neon at a PR of 3. Both fluids show slight increases, reaching around 770 kW and 780 kW, respectively, at a PR of 4. These results indicate significant thermodynamic inefficiencies for these fluids compared to the others.

Figure 13 shows the energy efficiency of fluids as a function of the PR, ranging from 3 to 4. The results reveal distinct trends for each fluid, with variations in efficiency across the PR range. Carbondioxide demonstrates the highest energy efficiency among the fluids, starting at approximately 29% at a PR of 3 and increasing slightly to around 32% at a PR of 4. This consistent improvement with rising PRs highlights carbondioxide's superior thermodynamic performance. Nitrogen and argon exhibit similar energy efficiency levels, though nitrogen slightly outperforms argon. Nitrogen maintains an efficiency of approximately 18%, remaining nearly constant across the PR range. Argon's efficiency starts at about 18% and decreases marginally to 15%, indicating stable but slightly declining performance. Helium and neon show the lowest energy efficiencies, with helium slightly outperforming neon. Helium begins at around 15% and gradually decreases to approximately 14%, while neon starts at 14%

and reduces to about 13%. These trends suggest higher irreversibilities for these fluids compared to the others. Figure 14 depicts the exergy efficiency of five fluids—helium, carbondioxide, nitrogen, argon, and neon—across a range of PRs from 3 to 4. The trends indicate varying performance levels for the fluids, with carbondioxide consistently outperforming the others. Carbondioxide exhibits the highest exergy efficiency, starting at approximately 44% at a PR of 3 and increasing to around 47% at a PR of 4. This consistent improvement underscores its thermodynamic advantage in minimizing irreversibilities. Nitrogen and argon have similar efficiencies, with nitrogen slightly ahead. Nitrogen maintains a nearly constant efficiency of 26%, while argon decreases marginally from 26% to 23% as the PR increases. Helium and neon demonstrate the lowest efficiencies among the fluids. Helium starts at around 22% and drops slightly to 18%, while neon begins at 21% and reduces to approximately 17%, indicating significant thermodynamic losses. In summary, carbondioxide stands out as the most efficient working fluid, while helium and neon lag due to higher irreversibilities. Nitrogen and argon provide moderate and stable performance, making them viable for systems requiring balanced exergy efficiency.

Figure 15 shows the variation in mass flow rate for five fluids across a PR range of 3 to 4. The trends highlight how each fluid responds to increasing PRs in terms of mass flow requirements. Argon demonstrates the highest mass flow rate, starting at approximately 10 kg/s at a PR of 3 and decreasing slightly to around 9 kg/s at a PR of 4. This indicates its significant density and energy transport capacity. Nitrogen maintains a consistent mass flow rate of approximately 6 kg/s, with negligible changes as the PR increases. Neon exhibits a mass flow rate close to 5 kg/s, remaining nearly constant across the PR range. Carbondioxide shows a stable mass flow rate of around 5 kg/s, reflecting its excellent heat transfer characteristics and lower mass requirement compared to other fluids. Helium consistently maintains the lowest mass flow rate, approximately 1 kg/s, throughout the entire PR range.

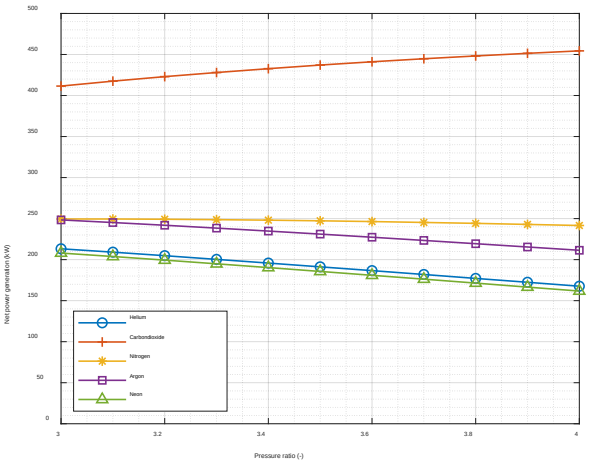

Figure 11. Effect of PR on net power.

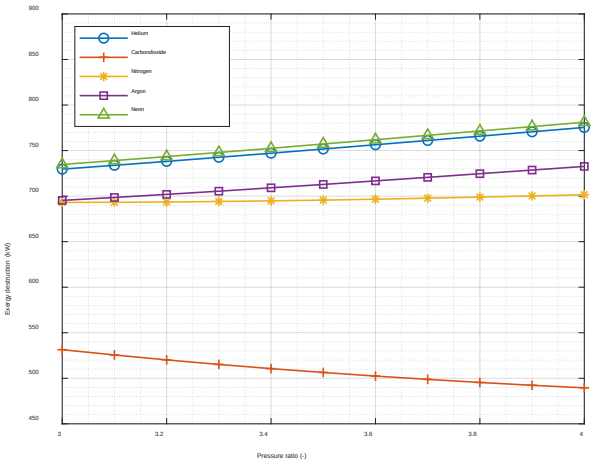

Figure 12. Effect of PR on exergy destruction.

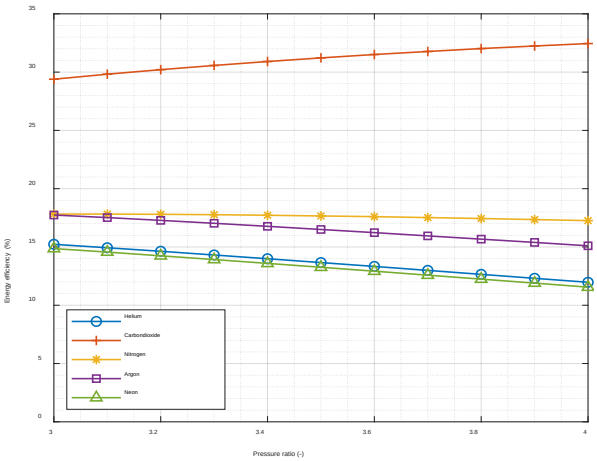

Figure 13. Effect of PR on energy efficiency.

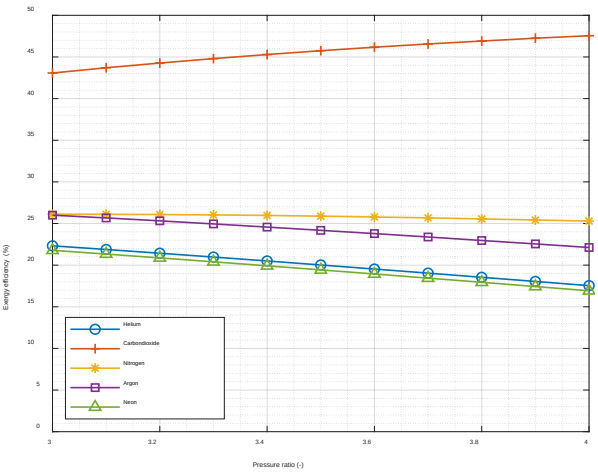

Figure 14. Effect of PR on exergy efficiency.

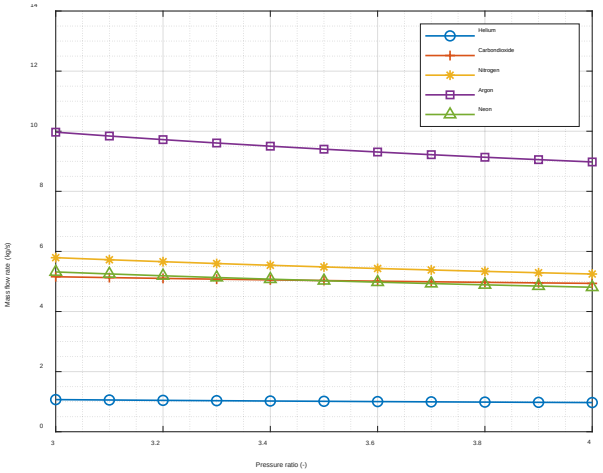

Figure 15. Effect of PR on mass flow rate.

Figure 16 shows the net power generation of five fluids at varying compressor inlet temperatures from 34°C to 54°C. The trends demonstrate how increasing the compressor inlet temperature impacts the performance of each fluid. Carbondioxide achieves the highest net power generation among the fluids, starting at approximately 440 kW at 34°C and decreasing slightly to around 430 kW at 37°C. This decrease indicates a small loss in efficiency as the compressor inlet temperature increases. Nitrogen begins with a relatively high-power output of approximately 250 kW at the lowest compressor inlet temperature of 34°C. As the compressor inlet temperature increases, nitrogen's net power generation decreases slightly, reaching a value close to 200 kW at the highest temperature of 54°C. Argon starts at approximately 230 kW and decreases slightly to 160 kW, showing a minor decline in performance. Neon and helium exhibit lower power generation levels compared to the other fluids. Neon begins at around 180 kW at 34°C and decreases slightly to about 130 kW at 54°C. Similarly, helium starts at 190 kW and drops to approximately 140 kW as the temperature rises.

Figure 17 indicates the exergy destruction trends for five working fluids—helium, carbondioxide, nitrogen, argon, and neon—across compressor inlet temperatures ranging from 34°C to 54°C. The trends reveal how increasing inlet temperature impacts exergy destruction in the system. Helium and neon exhibit the highest exergy destruction values among the fluids. Helium starts at approximately 750 kW at 34°C and increases slightly to around 810 kW at 54°C. Similarly, neon begins at 760 kW and rises to approximately 815 kW over the temperature range. These results indicate significant thermodynamic losses for these fluids compared to others. Argon and nitrogen demonstrate moderate levels of exergy destruction. Argon starts at around 710 kW at 34°C and increases slightly to approximately 760 kW at 54°C. Nitrogen starts with an exergy destruction value of approximately 700 kW at a compressor inlet temperature of 34°C. As the compressor inlet temperature increases to 54°C, the exergy destruction remains relatively stable, showing only a slight increase to around 740 kW. Carbondioxide exhibits the lowest exergy destruction among all working fluids, starting at approximately 500 kW at a compressor inlet temperature of 34°C and gradually increasing to about 560 kW at 54°C.

Figure 18 exhibits the energy efficiency trends of five working fluids across compressor inlet temperatures ranging from 34°C to 54°C. The results indicate a gradual decrease in energy efficiency for all fluids as the compressor inlet temperature increases. Carbondioxide maintains the highest energy efficiency among the fluids, starting at approximately 31% at 34°C and decreasing slightly to around 28% at 54°C. This minor decline reflects its strong thermodynamic performance and resilience to increased inlet temperatures. Nitrogen and argon show moderate efficiency levels, with nitrogen slightly outperforming argon. Helium and neon exhibit the lowest energy efficiencies. Helium starts at approximately 14% and drops to around 14%, while neon begins at 13% and declines slightly to 9% over the same temperature range. These trends highlight the limited energy conversion capabilities of these fluids compared to the others.

Figure 19 illustrates the exergy efficiency trends of five working fluids across compressor inlet temperatures ranging from 34°C to 54°C. The trends indicate that exergy efficiency decreases for all fluids as the inlet temperature increases. Carbondioxide maintains the highest exergy efficiency, starting at approximately 46% at 34°C and gradually decreasing to around 40% at 34°C. This performance highlights its strong thermodynamic properties and minimal irreversibility compared to the other fluids. Nitrogen and argon show moderate exergy efficiencies, with nitrogen slightly outperforming argon. Nitrogen begins at around 26% and decreases slightly to about 21%, while argon starts at 25% and drops to approximately 17% as the inlet temperature rises. Helium and neon exhibit the lowest exergy efficiencies, with helium slightly higher than neon. These results reflect their higher irreversibilities and lower thermodynamic performance.

Figure 20 represents the mass flow rate trends of five fluids over compressor inlet temperatures. The trends show how the mass flow rate remains mostly stable across this temperature range for all fluids. Argon has the highest mass flow rate, starting at around 9 kg/s and showing a slight increase to approximately 10 kg/s as the compressor inlet temperature increases. This consistent trend indicates argon's suitability for systems requiring high energy transport. Nitrogen has a consistent mass flow rate of approximately 5.5 kg/s across the entire temperature range. Neon closely follows nitrogen, maintaining a mass flow rate of around 5 kg/s, showing a similar level of stability. Carbondioxide has a mass flow rate of approximately 5 kg/s, remaining constant over the range of temperatures. Helium has the lowest mass flow rate, consistently at 1 kg/s across the temperature range. This reflects its low density and high specific heat, allowing efficient heat transfer with minimal mass.

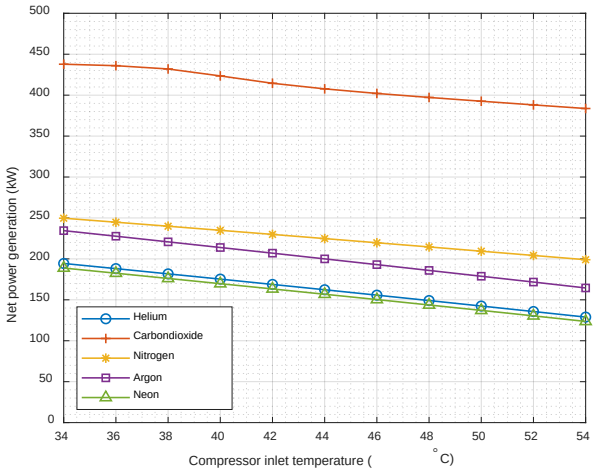

Figure 16. Effect of compressor inlet temperature on net power generation.

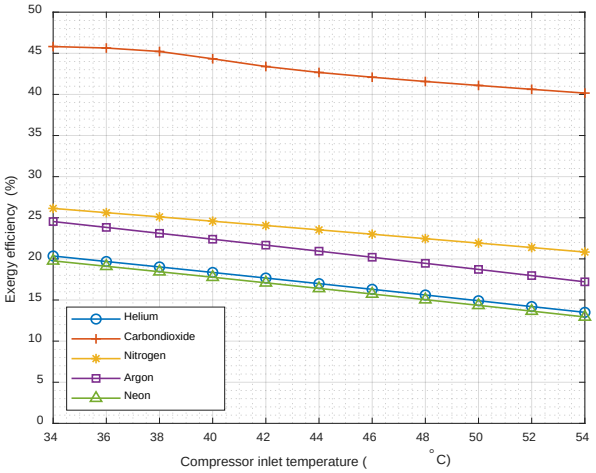

Figure 19. Effect of compressor inlet temperature on exergy efficiency.

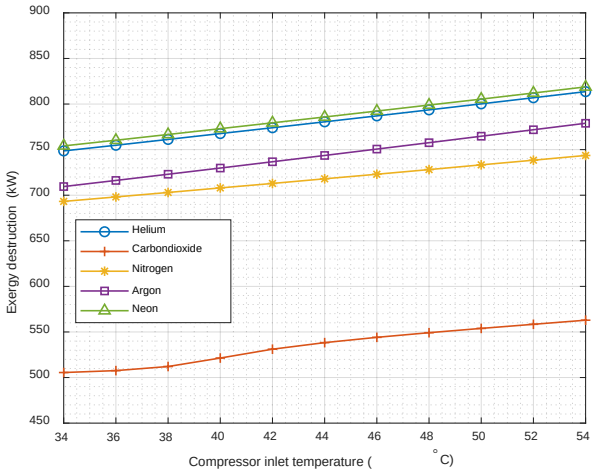

Figure 17. Effect of compressor inlet temperature on exergy destruction.

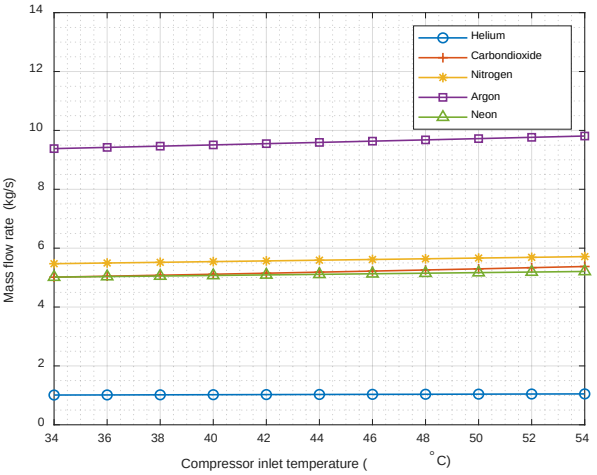

Figure 20. Effect of compressor inlet temperature on mass flow rate.

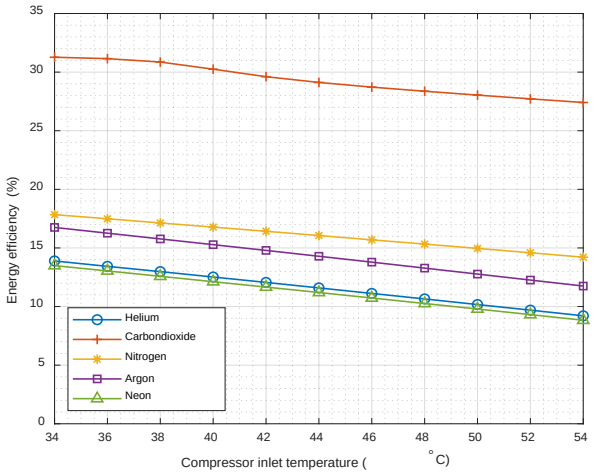

Figure 18. Effect of compressor inlet temperature on energy efficiency.

6. Conclusions

The objective of this study was to evaluate the thermodynamic performance of a power generation system employing different working fluids—helium, carbondioxide, nitrogen, argon, and neon—under varying operational parameters. By analyzing key performance metrics such as net power generation, exergy destruction, energy and exergy efficiencies, and mass flow rates, this research aimed to identify the most suitable working fluid for maximizing efficiency and minimizing energy losses in thermodynamic systems. The findings provide a comparative framework for the selection and optimization of working fluids in power generation applications.

- ✓Carbondioxide consistently demonstrated the best thermodynamic performance, achieving the highest net power generation of 450 kW and the lowest exergy destruction of 500 kW. It also maintained the highest energy efficiency (31%) and exergy efficiency (45%) across all conditions, making it the most suitable working fluid for high-performance systems.
- ✓Nitrogen and argon showed balanced thermodynamic behavior, with net power generation values of around

250 kW and 230 kW, respectively. Exergy destruction for these fluids ranged between 700–720 kW, and their energy and exergy efficiencies remained moderate at 17% and 25%, respectively, highlighting their suitability for applications requiring stable and reliable operation.

- ✓Neon and helium exhibited lower performance metrics, with neon achieving the lowest net power generation (170 kW) and helium showing slightly higher values (180 kW). Both fluids also had high exergy destruction levels, exceeding 770 kW, and reduced energy (13%) and exergy efficiencies (19%), indicating significant thermodynamic limitations.
- ✓The mass flow rate analysis revealed that argon required the highest flow rate (9.5 kg/s), reflecting its high density and energy transport needs. Helium, with the lowest flow rate (1 kg/s), demonstrated reduced energy transport capacity, limiting its application for high-efficiency systems.
- ✓Increasing turbine inlet temperature improved net power generation and efficiencies for all fluids, while higher compressor inlet temperatures led to a decline in performance metrics.

This study highlights the thermodynamic performance of various working fluids in a Closed Brayton Cycle system integrated with waste heat recovery. The findings demonstrate significant advantages, such as improved energy efficiency, reduced exergy destruction, and the identification of optimal working fluids for enhanced power generation. These outcomes provide valuable insights for industries seeking to maximize energy recovery from waste heat sources, contributing to both operational cost savings and environmental sustainability. The benefits of this research extend to advancing the design of efficient power systems and promoting the use of sustainable energy solutions. Future studies will focus on experimental validation of the results and the exploration of hybrid configurations, such as integrating Organic Rankine Cycles, to further optimize system performance.

Author Contributions

The percentages of the author' contributions are presented below. The author reviewed and approved the final version of the manuscript.

	G.S.
C	100
D	100
S	100
DCP	100
DAI	100
L	100
W	100
CR	100
SR	100
PM	100
FA	100

C=Concept, D= design, S= supervision, DCP= data collection and/or processing, DAI= data analysis and/or interpretation, L= literature search, W= writing, CR= critical review, SR= submission and revision, PM= project management, FA= funding acquisition.

Conflict of Interest

The author declared that there is no conflict of interest.

Ethical Consideration

Ethics committee approval was not required for this study because of there was no study on animals or humans.

References

Alzuwayer B, Alhashem A, Albannag M, Alawadhi K. 2024. Advancements in supercritical carbon dioxide Brayton cycle for marine propulsion and waste heat recovery. Processes, 12: 1956.

Andreasen JG, Larsen U, Knudsen T, Pierobon L, Haglind F. 2014. Selection and optimization of pure and mixed working fluids for low grade heat utilization using organic Rankine cycles. Energy, 73: 204-213.

Angelino G, Invernizzi CM. 2011. The role of real gas Brayton cycles for the use of liquid natural gas physical exergy. Appl Therm Eng, 31: 827-833.

Arslan M, Yılmaz C. 2022. Design and optimization of multigeneration biogas power plant using waste heat recovery System: A case study with energy, exergy, and thermoeconomic approach of Power, cooling and heating. Fuel, 324: 124779.

Bejan A, Tsatsaronis G, Moran M. 1996. Thermal Design & Optimization, Wiley-Interscience, 1st ed., pp: 560.

Campana F, Bianchi M, Branchini L, De Pascale A, Peretto A, Baresi M. 2013. ORC waste heat recovery in European energy intensive industries: energy and GHG savings. Energy Convers Manag, 76: 244–252.

Cengel YA, Boles MA. 2015. Thermodynamics: An Engineering Approach, McGraw-Hill Professional, 8th ed., pp: 946.

Chen Q, Hammond GP, Norman JB. 2016. Energy efficiency potentials: contrasting thermodynamic, technical, and economic limits for organic Rankine cycles within UK industry. Appl Energy, 164: 984–990.

Dincer I, Rosen MA. 2013. Exergy: Energy, environment and sustainable development, Elsevier Sci, 3rd ed., pp: 724.

Farrukh S, Wu D, Al-Dadah R, Gao W, Wang Z. 2023. A review of integrated cryogenic energy assisted power generation systems and desalination technologies. Appl Therm Eng, 221: 119836.

Hajabdollahi Z, Hajabdollahi F, Tehrani M, Hajabdollahi H. 2013. Thermo-economic environmental optimization of organic rankine cycle for diesel waste heat recovery. Energy, 63: 142–151.

Hu S, Yang Z, Li J, Duan Y. 2021. Thermo-economic analysis of the pumped thermal energy storage with thermal integration in different application scenarios. Energy Convers Manag, 236: 114072.

Jafari M, Khan MM, Al-Ghamdi SG, Jaworski AJ, Asfand F. 2023. Waste heat recovery in iron and steel industry using organic Rankine cycles. Chem Eng J, 477: 146925.

Kim DK, Lee JS, Kim J, Kim MS, Kim MS. 2017. Parametric study and performance evaluation of an organic Rankine cycle (ORC) system using low-grade heat at temperatures below 80 ℃. Appl Energy, 189: 55-65.

Li B, Wang SS, Wang K, Song L. 2020. Thermo-economic analysis of a combined cooling, heating and power system based on carbondioxide power cycle and absorption chiller for waste heat recovery of gas turbine. Energy Convers Manag, 224: 113372.

Mocanu G, Losifescu C, Lon L.V, Popescu F, Fratita M, Chivu RM. 2024. Energy analysis of waste heat recovery using supercritical CO_2 Brayton cycle for series hybrid electric vehicles. Energies, 17: 2494.

Petr P, Raabe G. 2015. Evaluation of R-1234ze(Z) as drop-in replacement for R245fa in Organic Rankine Cycles-From

thermophysical properties to cycle performance. Energy, 93: 266-274.

Rad EA, Tayyeban E, Assareh E, Riaz A, Hoseinzadeh S, Lee M. 2024. Thermodynamic feasibility and multi-objective optimization of a closed Brayton cycle-based clean cogeneration system. J Therm Anal Calorim, 149: 1199-1218.

Salmi W, Vanttola J, Elg M, Kuosa M, Lahdelma R.2017. Using waste heat of ship as energy source for an absorption refrigeration system. Appl Therm Eng, 115: 501-516.

Yang S, Deng C, Liu Z. 2019. Optimal design and analysis of a cascade $LiBr/H_2O$ absorption refrigeration/transcritical CO_2 process for low-grade waste heat recovery. Energy Convers Manage, 192: 232–242.

Yilmaz F, Ozturk M, Selbas R. 2019. Design and thermodynamic analysis of coal-gasification assisted multigeneration system with hydrogen production and liquefaction. Energy Convers Manag, 186: 229–40.

Zhao P, Wang J, Gao L, Dai Y. 2012. Parametric analysis of a hybrid power system using organic Rankine cycle to recover waste heat from proton exchange membrane fuel cell. Int J Hydrogen Energy, 37: 3382–3391.

Xu J, Yu. 2014. Critical temperature criterion for selection of working fluids for subcritical pressure Organic Rankine cycles. Energy, 74: 719–733.